

Supporting Information

Adaptive coloration enabled by the reversible osmotic annealing of chromatophore-like microcapsules

Jae-Hyun Kim,^{‡a} Ji-Young Lee,^{‡b} Jaekyoung Kim,^{‡a} Zhe Gong,^a Daniel J. Wilson,^c Leila F. Deravi^{*b} and Daeyeon Lee^{*a}

[‡]These authors contributed equally to this work

***Corresponding authors**

Email address: daeyeon@seas.upenn.edu (D. Lee), l.deravi@northeastern.edu (L. F. Deravi)

^a Department of Chemical and Biomolecular Engineering, University of Pennsylvania
Philadelphia, PA 19104, United States

^b Department of Chemistry and Chemical Biology, Northeastern University, Boston, MA 02115,
United States

^c Kostas Research Institute, Northeastern University, Burlington, MA 01803, United States

KEYWORDS: colloidal photonic glass, pigment, bio-inspired, structural color, confined colloid assembly, osmotic pressure.

Supporting Figures and Table

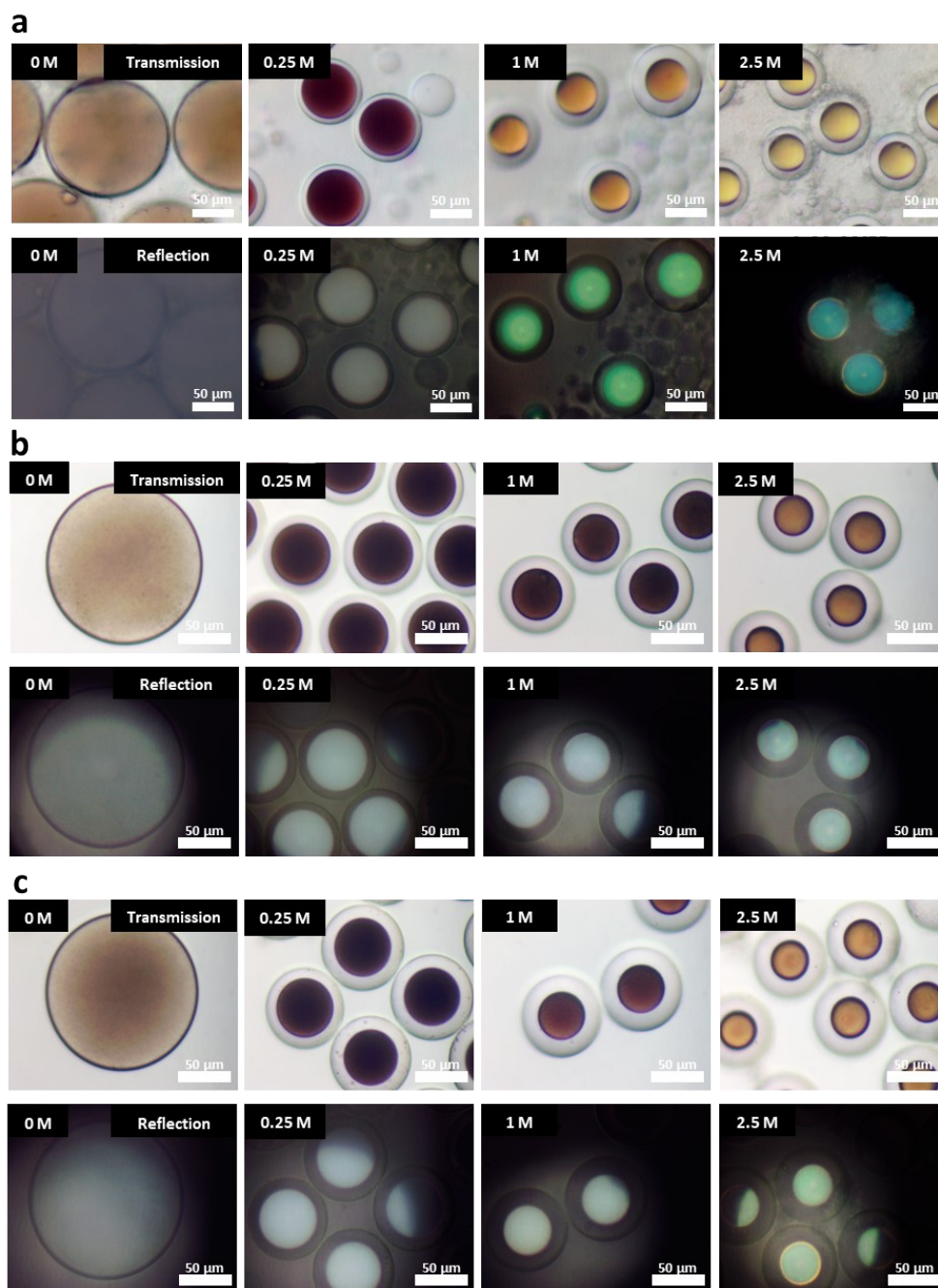


Figure S1. Fabrication of reversible color changing capsules. Optical microscope images of photonic capsules annealed via different salt concentrations (0 M – 2.5 M). Images from (a) PS nanoparticles annealed within double emulsion capsules and (b-c) varying densities of Xa-loaded onto PS nanoparticles. Here, (b) represents double emulsion capsules containing a low density of Xa (Xa1) and (c) represents double emulsion capsules containing a high density of Xa (Xa2).

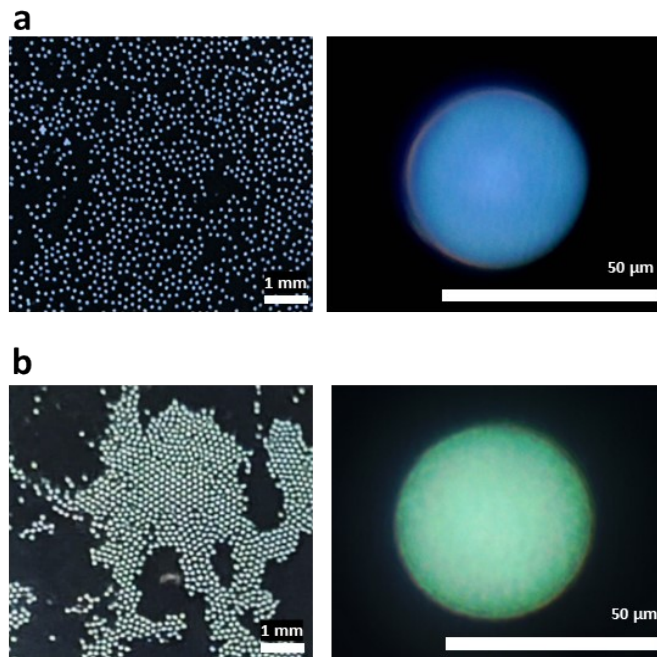


Figure S2. Addition of osmolyte to the inner phase of double emulsions for enabling swelling inner phase. Optical image of osmosis annealed double emulsion capsules and optical microscope reflection mode image of annealed photonic core part. (a) None-reversible (sucrose 0 mM) PS double emulsions and (b) reversible (sucrose 50 mM) PS double emulsions.

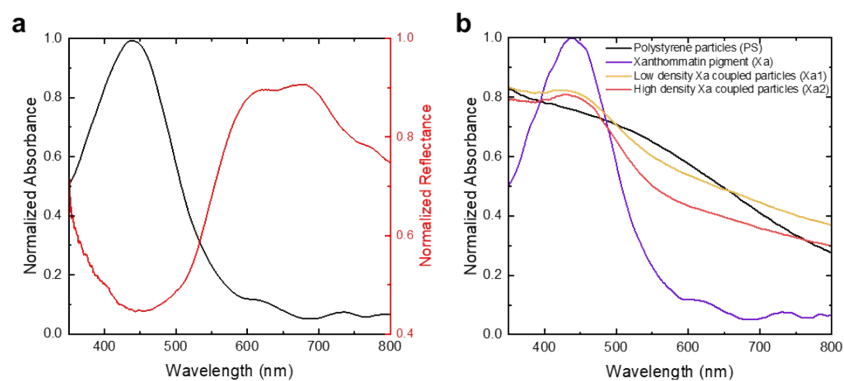


Figure S3. (a) Normalized absorbance and reflectance spectrum of pigment (Xa). (b) Normalized absorbance spectra of PS, Xa1, and Xa2 particles to the Xa pigment. All particles and pigment are suspended in DI water for absorbance measurement and drop-casted onto glass slides for reflectance measurement. Spectrum is normalized by the maximum absorbance in the range of 300 – 800 nm.

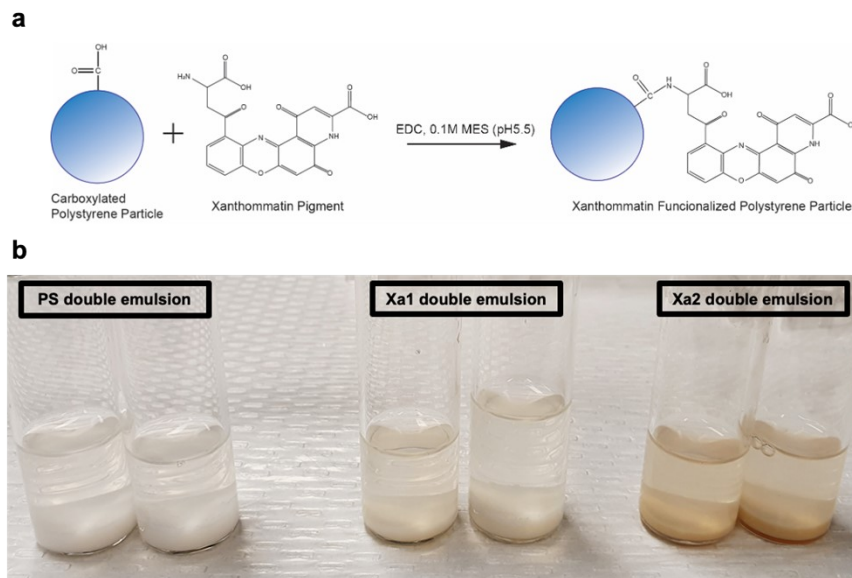


Figure S4. (a) Schematic diagram of Xa coupling to PS. (b) Images of photonic capsules containing varying densities of Xa on PS. The fabricated double emulsion is stable over several months in 5wt.% PVA aqueous solution. As the loaded pigment density increases, the double emulsion color becomes brown. Xa2 double emulsion is fabricated with the highest pigment density. (a) Schematic diagram of Xa coupling to PS. (b) Images of photonic capsules containing varying densities of Xa on PS. The fabricated double emulsion is stable over several months in 5wt.% PVA aqueous solution. As the loaded pigment density increases, the double emulsion color becomes brown. Xa2 double emulsion is fabricated with the highest pigment density.

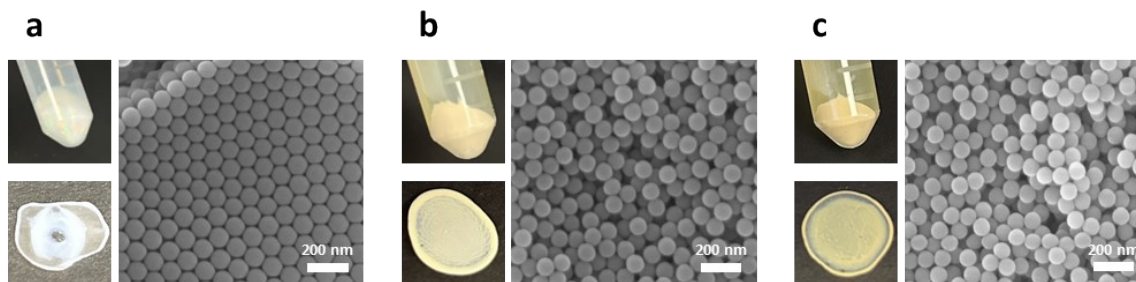


Figure S5. The photograph of centrifuged solution and samples prepared by drop casting technique for SEM image of nanoparticles. a) PS, b) Xa1 and c) Xa2.

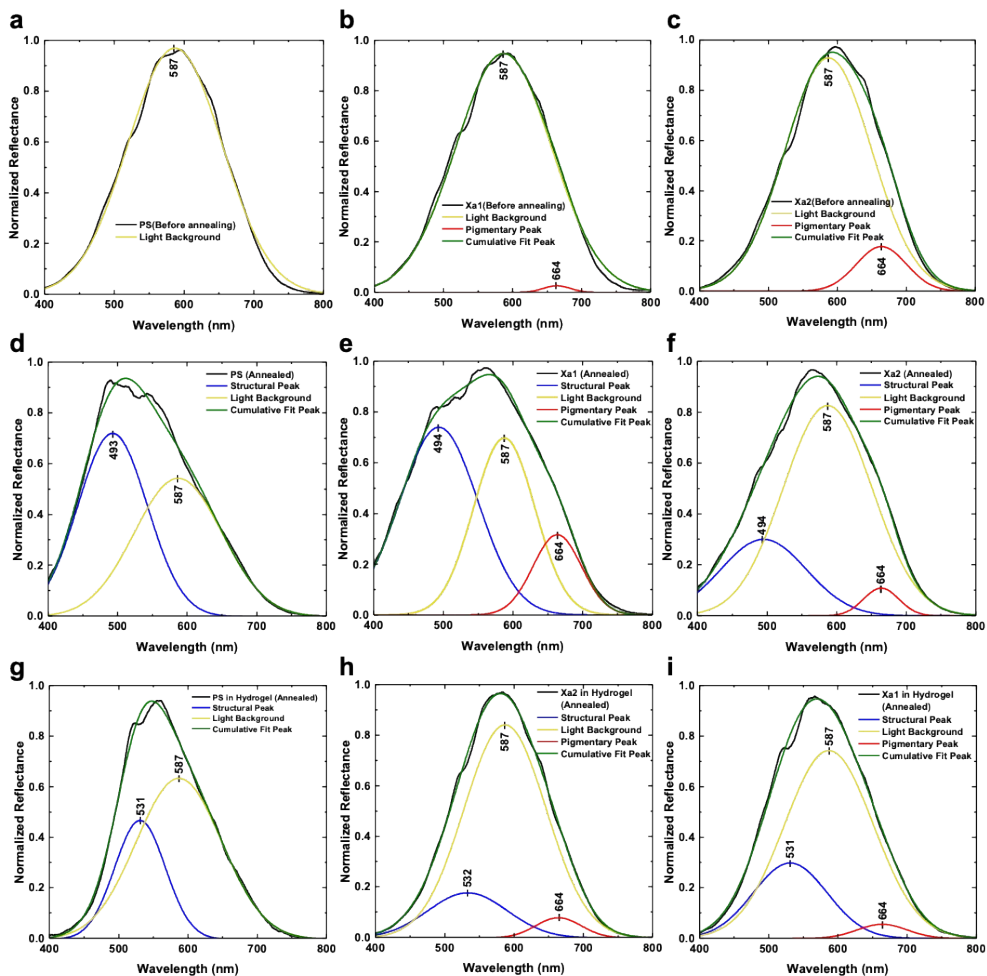


Figure S6. Deconvoluted reflectance spectra of microcapsules. (a-c) Before annealing of PS, Xa1, and Xa2 microcapsules. (d-f) Osmotically annealed PS, Xa1, and Xa2 microcapsules. (g-i) Osmotically annealed PS, Xa1, and Xa2 microcapsules in hydrogel matrix.

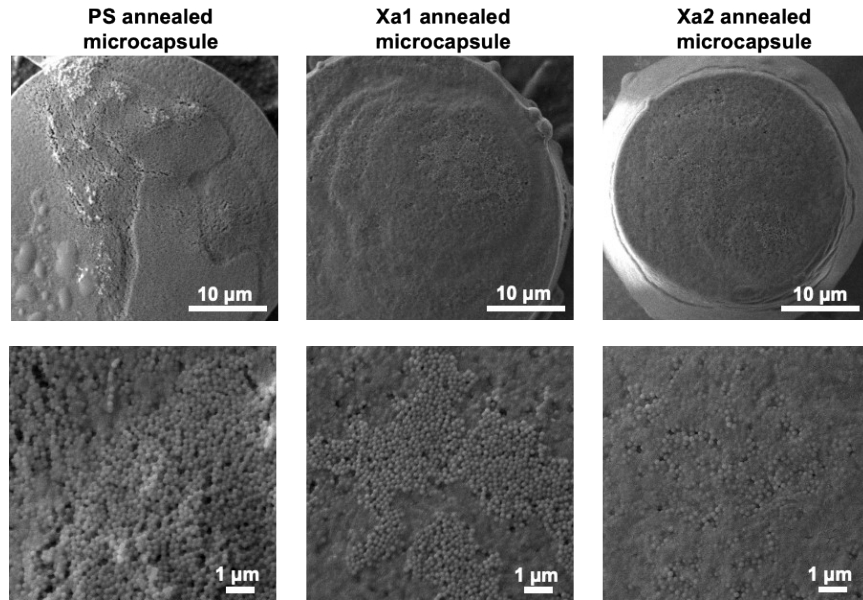


Figure S7. SEM images of the annealed photonic capsules.

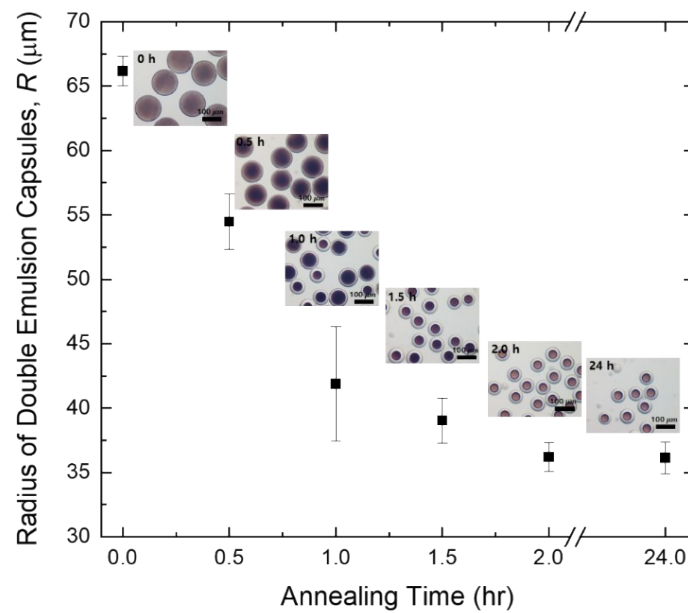


Figure S8. Radius of Xa2 double emulsion capsules over annealing time with microscope image.

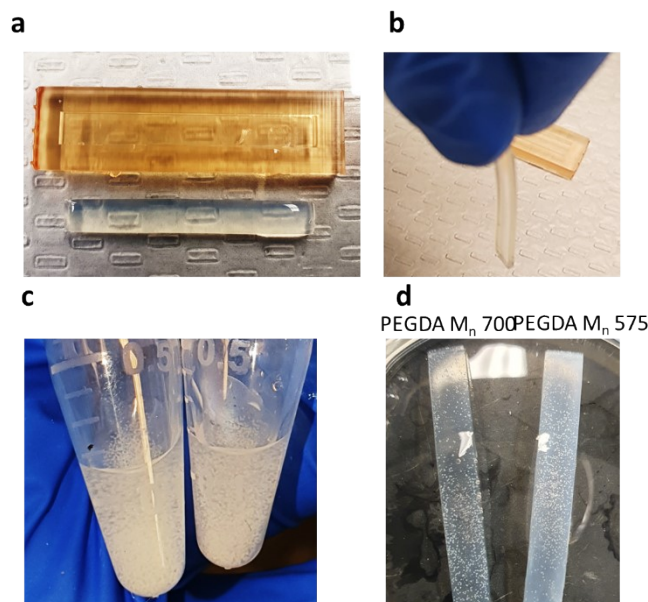


Figure S9. Fabrication of Artificial Cephalopod Skin: The hydrogel matrix was created using Poly(ethylene glycol) diacrylate (PEGDA) and the photo-crosslinker lithium phenyl-2,4,6-trimethylbenzoylphosphinate (TPO-Li). (a) A 3D-printed mold (2cm × 1cm × 1.2cm) was employed to control the hydrogel's morphology. (b) After UV-crosslinking for 20 seconds, the hydrogel could be easily detached from the mold. (c) The fabricated double emulsion was mixed effectively with the PEGDA and TPO-Li aqueous solution. This solution was then added to the 3D-printed mold to fabricate the hydrogel. (d) The resulting artificial cephalopod skin was immersed in a salt solution, and it was observed that hydrogel matrix using PEGDA with Mn 700 exhibited better transmittance compared to the one using PEGDA with Mn 575. We speculate that PVA aggregates more readily in PEGDA with Mn 575.

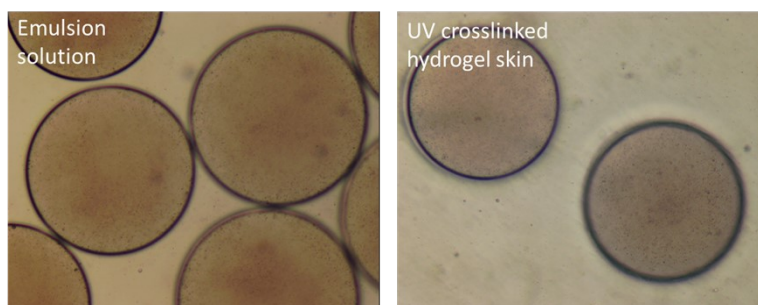


Figure S10. Optical microscope image comparison after hydrogel cured. The Xa2 particles are in the inner phase, and after UV-crosslinking the PEGDA hydrogel, the double emulsions show good stability. We could observe after the UV-crosslinking the edge of the emulsions seem to attach very well to the hydrogel.

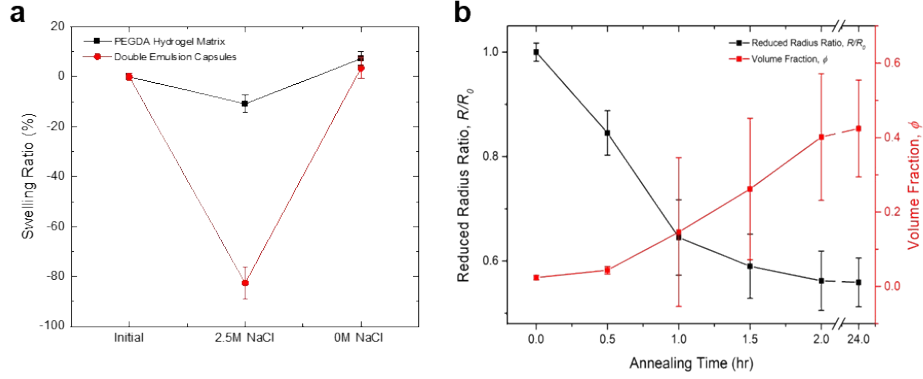


Figure S11. (a) Swelling ratio for PEGDA hydrogel and photonic microcapsules embedded in the hydrogel. The swelling ratio is calculated by taking the weight difference of hydrogel between initial and 2.5 M NaCl or initial and 0 M NaCl and then dividing it by the initial weight. (b) Normalized radius (R/R_0) of Xa2 microcapsules in hydrogel over annealing time (2.5 M NaCl with 2.5 wt.% PVA) and volume fraction of Xa2 microcapsules in hydrogel over annealing time.

Table S1. Zeta Potential (mV) of polystyrene (PS), low-density Xa coupled with PS (Xa1) and high-density Xa coupled with PS (Xa2) in different solutions were measured with dynamic light scattering (DLS).

	In water	In Sucrose 50mM + PVA 0.5wt%
PS	-52.2 ± 1.86	-6.69 ± 1.51
Xa1	-9.56 ± 1.76	-4.75 ± 0.92
Xa2	-7.37 ± 1.94	-5.28 ± 0.83

Supporting Equations for Photonic Crystal and Photonic Glass Structure

If we consider the annealed microcapsules as photonic crystals, reflectance wavelength can be approximated using the following equation [1-3].

$$\lambda = 2dn_{eff} = \left(\frac{\pi}{3\sqrt{2}\phi}\right)^{1/3} \left(\frac{8}{3}\right)^{1/2} D \{n_{PS}^2\phi + n_{med}^2(1-\phi)\}^{1/2}$$

where d is the lattice spacing, n_{eff} is the effective refractive index, ϕ is the volume fraction of particles, D ($= 170$ nm) is the particle diameter, n_{PS} ($= 1.59$) is the PS particles refractive index, and n_{med} is the refractive index of the medium in the inner phase. In our experiments, the refractive index of the particle remains constant during osmotic annealing, whereas the volume fraction of particles (ϕ) and refractive index of medium in the inner phase of double emulsion change,

resulting in the shift of the wavelength of Bragg reflection. After annealing, the volume fraction of particle is $\phi = 0.53 \pm 0.11$, the concentrations of sucrose and PVA in the inner phase become approximately 1 M and 11 wt.%, respectively, raising the refractive index of this medium to $n_{med} = 1.4$. Thus, the calculated wavelength using this equation for photonic crystal structure provides a range of 444 - 495 nm.

If we consider the annealed microcapsules as photonic glasses, wavelength can be estimated using the following equation [4].

$$\lambda = \left(\frac{4\pi n_{eff} d}{x_0} \right) \sin\left(\frac{\theta}{2}\right)$$

where n_{eff} is the effective refractive index, d is the diameter of the particles, $x = qd$ is the dimensionless wavevector.

Structure factor is calculated using the Ornstein-Zernike equation for the hard-sphere potential under the Percus-Yevick approximation method. The volume fraction is computed to be 0.53, with a diameter of 170 nm [5].

$$S_1(q) = \frac{1}{1 + 24\phi G(R_{HS}q)/(R_{HS}q)}$$

$G(A)$

$$= \frac{\alpha(\sin A - A \cos A)}{A^2} + \beta(2A \sin A + (2 - A^2) \cos A - \frac{2}{A^3}) + \gamma \frac{[-A^4 \cos A + 4|(3A^2 - 6) \cos A]}{A^5}$$

$$\alpha = (1 + 2\phi)^2 / (1 - \phi)^4$$

$$\beta = -6\phi(1 + \frac{\phi}{2})^2 / (1 - \phi)^2$$

$$\gamma = \phi\alpha/2$$

where R_{HS} is the hard-sphere radius, ϕ is the volume fraction of hard-sphere.

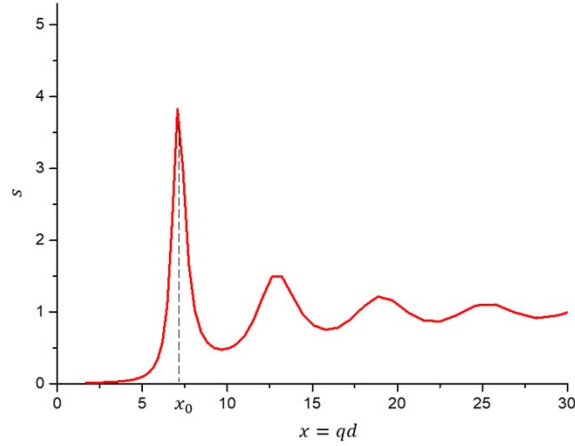


Figure. S12. Structure factor of a colloidal glass with volume fraction $\phi=0.53$ calculated from the Ornstein-Zernike equation under the Percus-Yevick approximation.

The value of x_0 is the first peak in the structure factor. $q_0 = 0.004162$, $d = 170 \text{ nm}$, and $x_0 = 7.07504$. n_{eff} is obtained using the Maxwell-Garnett mean-field approximation as shown in the following equation.

$$n_{eff} = n_{med} \sqrt{\frac{2n_{med}^2 + n_p^2 + 2\phi(n_p^2 - n_{med}^2)}{2n_{med}^2 + n_p^2 - \phi(n_p^2 - n_{med}^2)}}$$

In our experiments, after annealing the medium refractive index is $n_{med} = 1.4$, particle refractive index is $n_{ps} = 1.59$, and volume fraction is $\phi = 0.53$. Then, the effective refractive index is calculated as $n_{eff} = 1.50$. The calculated reflection wavelength with photonic glass equations is in the range of 412 - 495 nm.

Reference

- [1] S. J. Yeo, F. Tu, S.-h. Kim, G.-R. Yi, P. J. Yoo and D. Lee, *Soft Matter*, 2015, 11, 1582-1588.
- [2] T. M. Choi, J.-G. Park, Y.-S. Kim, V. N. Manoharan and S.-H. Kim, *Chemistry of Materials*, 2015, 27, 1014-1020
- [3] P. A. Rundquist, P. Photinos, S. Jagannathan and S. A. Asher, *The Journal of Chemical Physics*, 1989, 91, 4932-4941.
- [4] J. S. Pedersen, *Advances in Colloid and Interface Science*, 1997, 70, 171-210.
- [5] S. Magkiriadou, J.-G. Park, Y.-S. Kim and V. N. Manoharan, *Physical Review E*, 2014, 90, 062302.